J Mater Sci: Mater Electron (2017) 28:15685–15693
DOI 10.1007/s10854-017-7458-5

CrossMark

Non-ohmic properties of $CaCu_3Ti_4O_{12}$ thin films deposited By RF-sputtering

C. R. Foschini[1] · B. Hangai[3] · C. S. Cavalcante[3] · A. Z. Simões[3] · M. Cilense[2] · E. Longo[2]

Received: 10 May 2017 / Accepted: 1 July 2017 / Published online: 14 July 2017
© Springer Science+Business Media, LLC 2017

Abstract Calcium copper titanate ($CaCu_3Ti_4O_{12}$, CCTO), thin films with polycrystalline nature have been deposited by RF sputtering on Pt/Ti/SiO_2/Si (100) substrates at a room temperature followed by annealing at 600 °C for 2 h in a conventional furnace. The CCTO thin film present a cubic structure with lattice parameter $a=7.379\pm0.001$ Å free of secondary phases. Dielectric spectroscopy was employed to examine the polycrystalline behaviour of CCTO material and the mechanisms responsible for the barrier-layer capacitances associated with Schottky-type barriers and the non-Ohmic properties. The film presents an electric breakdown field ($E_b=203$ V cm^{-1}) and then nonlinear coefficient ($\alpha=6$), which is even lower than that of the ZnO and SnO_2 based varistors The observed electrical features of CCTO thin films are highly dependent on the [CaO_{12}], [CaO_4], [CuO_{11}], [$CuO_{11}V_o^x$] and [$TiO_5 \cdot V_O^{\bullet}$] clusters.

1 Introduction

The nonlinear current–voltage (*I*–*V*) behaviour [1] of calcium copper titanate (CaCu3Ti4O12, CCTO) ceramics undoubtedly has a great potential in the surge protection device industry. The first report [2] on varistor property of CCTO shows that an intrinsic electrostatic barrier built at the CCTO grain boundary is responsible for the nonlinear current voltage behaviour. In the CCTO polycrystalline ceramic, back-to-back potential barriers formed from band bending at the boundary region (like the *n-i-n* acceptor interface [3] electron trap, caused by negatively charged intrinsic donor defects) leads to an abrupt drop in potential from grain to grain boundary. This mechanism was further supported by Mei et al. [4] by a thorough study of grain and grain boundary composition. Their study reveals that a Cu-rich secondary phase at the grain boundary with negatively charged vacancies () is responsible for the double Schottky barriers (n-in) with the n-type semiconductor grain boundary and grains [5, 6].

Chung et al. reported that CCTO exhibits nonlinear current-voltage characteristics even in the absence of any dopants [7]. These outstanding electrical properties are quite unusual since CCTO exhibits a body centered cubic perovskite structure with slightly tilted [TiO_6] octahedra facing each other [8], i.e. the compound is not ferroelectric. Despite numerous studies including quantum chemical calculations [9], the origin of this high dielectric constant remains still unclear. Impedance spectroscopy has proven that such ceramics consist of semiconducting grains and insulating grain boundaries. Results from Sinclair et al. [3] suggest that the high dielectric constant is actually an internal grain boundary barrier layer capacitance, in other words, it is a grain boundary effect that is not linked to the perovskite crystal structure. Since the nonlinear electrical properties are not independent from the grain boundary nature, one would expect that they are somehow connected to the grain boundary barrier layer capacitance. It is also known that oxygen adsorbed at the grain boundaries plays

✉ A. Z. Simões
alezipo@yahoo.com

[1] Dept. de Eng. Mecânica, Faculdade de Engenharia de Bauru, Universidade Estadual Paulista, UNESP, Av. Eng. Luiz Edmundo C. Coube 14-01, Bauru, SP CEP 17033-360, Brazil

[2] Instituto de Química, Universidade Estadual Paulista, UNESP, Rua Prof. Francisco Degni nº 55, Araraquara, SP CEP 14800-900, Brazil

[3] Faculdade de Engenharia de Guaratinguetá, Universidade Estadual Paulista, UNESP, Av. Dr. Ariberto Pereira da Cunha, nº 333, Guaratinguetá, SP CEP 12516-410, Brazil

a fundamental role in the mecanism of a potential barrier formation. The literature contains numerous studies on the influence of heat treatments of varistor ceramics in reducing or oxidizing atmospheres on the electical properties [10, 11]. Capacitance measurements (10 Hz–1 MHz) on single crystals and ceramics have shown a high and relatively temperature independent permittivity value higher than 10,000 over a wide temperature range ~100–600 K. Below ~150 K, the permittivity drops rapidly to a value of ~100, but is not accompanied by any structural phase transition. To account for the dramatic decrease in permittivity below 150 K, it has been suggested that the dipoles ''freeze'' (relax out) at low temperatures. Besides their excellent piezoelectric and dielectries properties S. Y. Chung et al. observed by using Kelvin probe force microscopy that a large potential barrier intrinsically exists at the grain boundaries in addition to the intriguing dielectric response [12]. This behaviour serves as an obstacle to the current flow through the conductive bulk grains in a polycrystalline specimen, and thus results in enormous nonlinearity between the current and applied voltage. The same author demonstrated that, in addition to high permittivity, $CaCu_3Ti_4O_{12}$ has remarkably strong nonlinear current–voltage characteristics without the addition of any dopants. An intrinsic electrostatic barrier at the grain boundaries is responsible for the unusual nonlinear behaviour. The nonlinear coefficient $CaCu_3Ti_4O_{12}$ reaches a value of 900, which is even greater than that of the varistor material ZnO. As a result, $CaCu_3Ti_4O_{12}$ may lead to efficient switching and gas-sensing devices. However, very little is know about the the chemical nature of grain boundary interfaces in this system and its relationship to non-ohmic electrical behaviour. Therefore, in this paper, the main goal is to discuss the nonlinear response of highly dense $CaCu_3Ti_4O_{12}$ non-ohmic polycrystalline film deposited on $Pt/TiO_2/SiO_2/Si$ substrates by RF sputtering, to gain a better understanding of the nature of trap states and the electrical characteristics of this class of non-ohmic polycrystalline ceramics. It is useful to fabricate CCTO thin films with high nonlinear coefficients which could be widely used as resistors or varistors for surge protection, both in electronic circuits and in power systems.

2 Experimental procedure

The CCTO targets were prepared by conventional solid state reaction. Calcium carbonate, copper oxide and titanium dioxide (>99% purity and <1 µm) were mixed by ball milling in ethanol for 12 h. After dried the powder was calcined at 900 °C for 12 h. The calcined powder was mixed with PVA as a binder and uniaxially pressed into discs of approximately 50 mm in diameter and 3 mm thickness and sintered at 1100 °C for 3 h. From these targets nanostructured $CaCu_3Ti_4O_{12}$ films deposited on $Pt/Ti/SiO_2/Si$ substrates were obtained by RF sputtering at room temperature. The target substrate distance was kept at 85 mm and temperature, atmosphere and deposition rate were controlled. The Ar deposition pressure was 50 mTorr with 150 W RF power. CCTO films were characterized by X-ray diffraction (XRD, Rigaku, Model Rint 2000) at 40 kV and 150 mA from 2θ (20–80°) following the phase evolution. The Rietveld analysis was performed with the Rietveld refinement program DBWS-941 1 [13]. The profile function used was the modified Thompson-Cox-Hastings pseudo-Voigt where η (the lorentzian fraction of the function) varies with the Gauss and Lorentz components of the full width at half maximum. The thickness of the annealed films was analyzed using a field emission gun scanning electron microscope (FEG-SEM, JEOL, Model 7500F). Atomic Force Microscopy technique was used to analyze the surface of the films (AFM, NanoScopeIIIa, Bruker).

The XPS analysis was carried out at a pressure of less than 10^{-7} Pa using a commercial spectrometer (UNI-SPECS UHV) to verify the changes in surface chemical composition of the treated specimens. The Mg K line was used (h = 1253.6 eV) and the analyzer pass energy was set to 10 eV. The inelastic background of the Cu 2p, Ca 2p, Ti 2p and O 1 s electron core-level spectra were subtracted using Shirley's method. The composition of the near surface region was determined with an accuracy of ±10% from the ratio of the relative peak areas corrected by Scofield's sensitivity factors of the corresponding elements. The spectra were fitted without placing constraints using multiple Voigt profiles. The width at half maximum (FWHM) varied between 1.2 and 2.1 eV and the accuracy of the peak position was ±0.1 eV. For electrical DC and AC measurements, top Au electrodes (diameter: 200 µm) were deposited by sputtering through a shadow mask at room temperature acquiring a metal-semiconductor-metal (MSM) capacitor configuration. Current-tension measurements were taken using a pulsed high voltage source (Keithley, Model 237). The breakdown electric field (E_b) was obtained at a current density of 1 mA cm^{-2}. The leakage current density was determined at an electric field equal to 70% of the breakdown field. The nonlinear coefficient (alpha) was obtained by curve-fitting the log J versus log E plot, using the equation $\log J = \alpha \times \log E + \log K$, i.e. the nonlinear coefficient alpha is the slope of the obtained straight line. Every single I–V curve was measured three times to ensure that the experimental data were reliable. It should be pointed out that the value of current was below 15 µA during all the measurements, so the thermal effect can be ignored. Measurements of real (C′) and the imaginary (C″) part of the complex capacitance were performed with a frequency response analyser (HP 4192) using frequencies ranging

from 100 Hz up to 1 MHz, with an amplitude voltage of 1 V.

3 Results and discussion

Figure 1 shows the X-ray diffraction pattern of the CCTO powder calcinated at 900 °C for 12 h. Besides the perovskite phase, no secondary phase was observed. Our XRD data confirm the presence of a cubic crystal system [14]. The Rietveld refinement of the powder, annealed at 600 °C for 2 h in a conventional furnace, can be seen in Fig. 1, along with an inset depicting CCTO crystal structure, with Ti atoms inside the octahedra, O atoms in the corners of the octahedra, Ca atoms in the corners of the network and Cu atoms in half of the inner edges. The major observed diffraction peaks correspond only to CCTO (JCPDF 01-075-2188). The calculated refinement and the difference between experimental data indicate a proper structural adjustment, as in accordance with the presented reported data [15]. No evidence of secondary phases, crystallographic symmetry lowering, and reflection splitting or superlattice reflections can be seen. The obtained results confirmed that the film crystallized in the pseudo-cubic phase, with no changes during the refinement. From the extremely low S value ($R_{wp}/R_{exp} = 1.4\%$), one can assume that the CCTO phase refinement was well performed. According to the XRD pattern, all diffraction peaks can

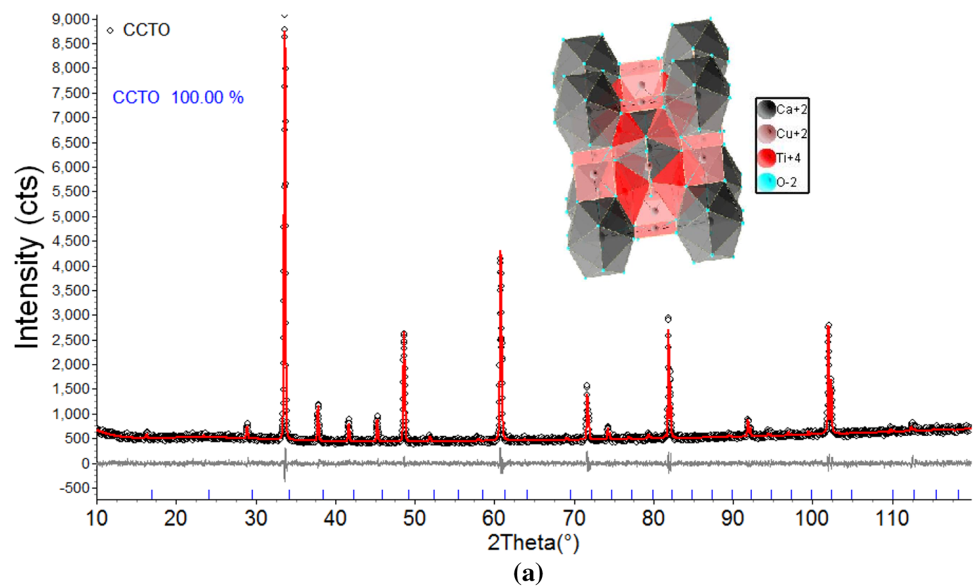

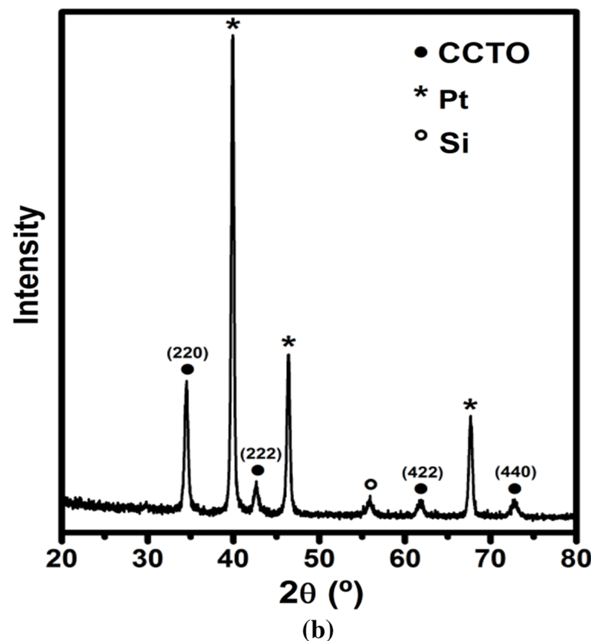

Fig. 1 **a** Rietveld refinement of CCTO powder, used to press the target for RF-sputtering deposition and *inset* showing its unit cell. **b** X-ray diffraction data for CCTO thin film deposited by RF sputtering at room temperature and annealed at 600 °C for 2 h in a conventional furnace

be indexed to $CaCu_3Ti_4O_{12}$. The characteristic peaks of Pt substrate can also be observed in the pattern. CCTO has a cubic structure with lattice parameter $a = 7.379 \pm 0.001$ Å. This is slightly less than the lattice parameter of CCTO reported previously [16]. This shows that the CCTO films can be prepared by the present process at much lower temperature than the solid state ceramic method. The lack of the peak at 49° can be explained by the low surface energy of the peak in the plane (004) due to its strain imposed by the cubic platinum substrate in the plane (111). This indicates that the as-prepared thin film is (h00)-oriented. Compared with the XRD intensity from the substrate, the intensity of the reflections from CCTO is obviously smaller. This is mainly due to the polycrystalline character as well as the relatively small thickness of the CCTO films.

In order to investigate the structural morphology of the CCTO film, a FEG-SEM image is depicted on Fig. 2, along with two insets showing its cross-sectional interface and its grain size distribution, obtained by AFM. Although no secondary phases were observed in FEG-SEM micrograph, electron dispersive spectroscopy revealed that the grain boundaries are CuO enriched relative to the interior of the grains. As can be seen, the grains present rounded morphology, uniformly distributed with an average mean grain size close to 13 nm. The majority of pores are nanostructured, with sizes around 5 nm, although larger pores could also be observed. The left inset shows a sharp interface between the CCTO film and the Pt substrate, with a film thickness of 606 nm. It's noteworthy to say that the homogeneous microstructure of CCTO film may reduce leakage current, enabling charge carriers to flow uniformly onto it [17]. A precipitate phase that is rich in Cu atoms and oxygen species can be viewed through an energy dispersive spectroscopy (EDS) stage attached to the scanning electron microscopy (SEM). The mapping of the oxygen element by EDS stage attached to FEG-SEM shows that the grain

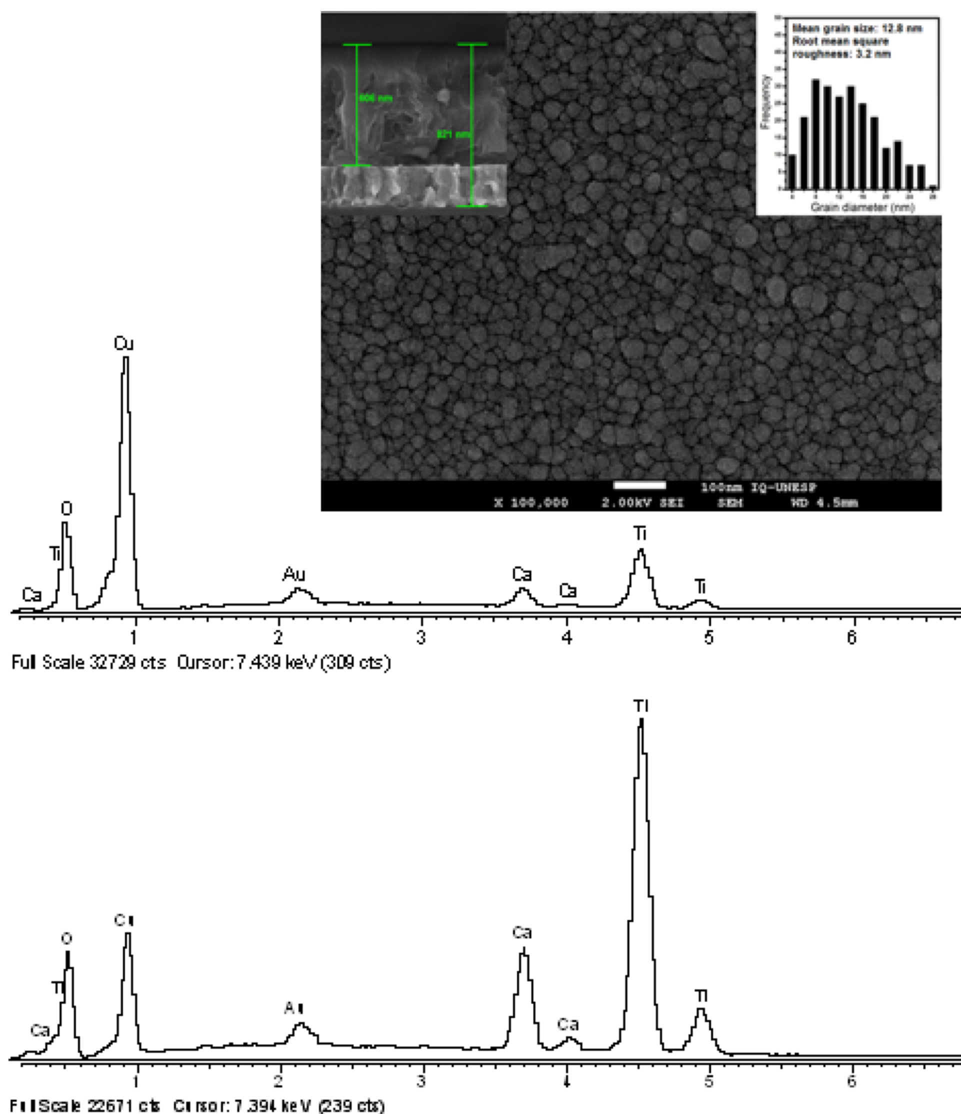

Fig. 2 FEG-SEM of the film surface after RF-sputtering, along with two *insets*: cross-sectional view (*left*) and grains size distribution (*right*). EDS analyses for a sintered CCTO sample: **a** grain boundary; **b** grain

boundary region is richer in oxygen than the grain is. The presence of precipitates at the grain boundaries is certainly important in defining the varistor behavior once prevents the mass transport through the grain boundaries, hindering the sintering process.

The XPS spectroscopy provided information on the bonding structure and composition of the near surface region of the material. The results of the quantitative analysis obtained for the as grown reference and samples prepared in oxygen and nitrogen atmosphere are listed in Table 1. Except the lower Ti content, the composition of the reference sample is close to the nominal stoichiometry of $CaCu_3Ti_4O_{12}$. The O_2 treatment led to an excess of Cu, due to Cu segregation o the surface forming copper oxide crystals. To get a better insight on the processes occurring on the surface, the evolution of the structural components was analyzed by the deconvolution of the Cu $2p_{3/2,}$ Ti $2p_{3/2}$ and Ca 2p spectra. The high-resolution Cu $2p_{3/2}$ spectra, displayed in Fig. 3c, show three distinct surface species, which were attributed to $CuCO_3$ (935.9 eV), CuO (934.4 eV) and Cu_2O (932.8 eV) [18]. The presence of copper carbonate was evidenced by the presence of the corresponding $CuCO_3$ component in the C 1 s spectra, found at about 288.6 eV (not shown). Despite the different treatment of the samples, the only difference observed is that the intensity of the main CuO component of the CCTO RF–O_2 sample decreases slightly on the expense of the Cu_2O subpeak. While for the reference sample the Ca 2p spectra indicate a pure CuO phase (834.8 eV), the CCTO RF–O_2 display a second spin–orbit component, indicating the formation of a $CaSO_4$ phase [18], due to the presence of sulphur, detected on the surface, Fig. 3a. Also the chemical bonding environment of Ti has been modified upon changed deposition conditions. The fitted Ti 2p spectra, displayed in Fig. 3b, show for the reference sample a principal component at about 458.4 eV, related to the TiO_2 phase, and a small high energy subpeak at 459.3 eV. The origin of the Ti 2p sub-peak is not quite clear, but is most probably related to oxygen vacancies forming fivefold coordinated sites in the TiO_2 lattice [19]. This is supported by the disappearance of this component for the sample prepared in the O_2 atmosphere.

Table 1 Atomic concentrations of CCTO RF samples treated in air, oxygen and nitrogen atmosphere

Element	CCTO RF	CCTO RF–O_2	CCTO RF–N_2
	Concentration (at. %)[a]		
Ca	5.3	4.9	7.1
Cu	14.1	20.4	13.2
Ti	14.3	12.3	15.4
O	66.2	61.1	62.5
S	–[b]	1.3	1.8

[a]Estimated error: ±10%

[b]Below the detection limit

Figure 4 shows the current density versus electric field plots obtained for a varistor films as-sintered. A mathematical analysis of the J×E curves leaded to somewhat different results, which are summarized in Table 2. It is interesting to note that the leakage current density is correlated linearly with the nonlinear coefficient (α). As it can be seen, high nonlinear coefficients correspond to low leakage currents when operating in the ohmic region, below

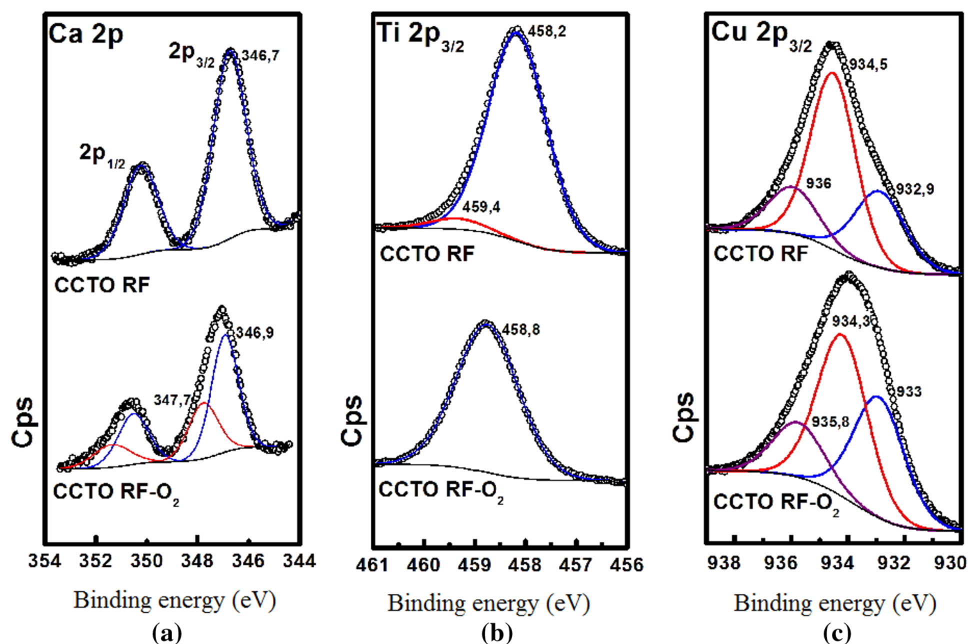

Fig. 3 XPS spectra for CCTO thin film deposited by the RF sputtering at room temperature and annealed at 600 °C for 2 h in a conventional furnace showing: **a** spin orbit doublets of Ca $2p_{3/2}$ and Ca $2p_{1/2}$, **b** Cu $2p_{3/2}$ and **c** Ti $2p_{3/2}$

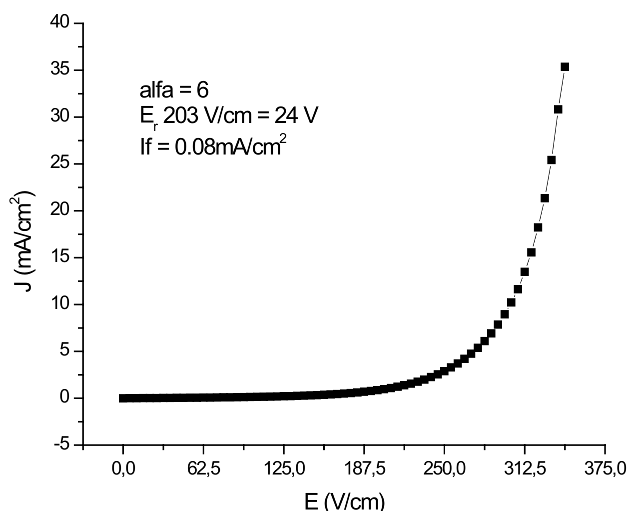

Fig. 4 Current density versus applied electric field for the varistor sample deposited by the RF sputtering at room temperature and annealed at 600 °C for 2 h in a conventional furnace

the breakdown electric field. An ideal varistor possesses an infinitely high (α) and does not present any leakage current indicating that the barrieres at the grain boundaries are extremely effective. When a varistor presents a pronounced transition range from the ohmic to the nonlinear region, which translates to a high leakage current and a low (α), a significant quantity of the grain boundary barriers is not effective. Therefore, the breakdown electric field is related to (α) and the barrier height. One can conclude that the previously desorbed oxygen is replaced by oxygen coming from the interior of the grains and that oxygen vacancies are created and are probably the main crystal defects in that ceramic. In that way, a deep insight in the barrier structure can be obtained. Also, from our previous work we suggest that Cu^{1+} is incorporate in the net of CCTO and probably substitutes part of Cu^{2+} generating electronic defects, which are compensated by oxygen vacancies. It is, therefore, assumed that Cu^{1+} is present in the CCTO crystalline structure as a point defect substituting Cu^{2+} and forming Cu'_{Cu} structural imperfections. The existence of two different Ti clusters, basically TiO_6 and $[TiO_5{\cdot}V_O^{\bullet}]$ can be explained considering the existence of species subcoordinated of titanium, in other words, clusters disordered associated to oxygen vacancies as $[TiO_5{\cdot}V_O^{\bullet}]$ [20]. The oxygen vacancies would be easily accommodated in the TiO_5 local substructure. Thus, the increasing of Cu–O bonding causes structural disorder in the TiO_6 octahedron network. The charge transfer between $[TiO_5{\cdot}V_O^{\bullet}]$ clusters and Cu'_{Cu} defects creates positive and negative polarons and the combination of both constitutes a new entity called Jahn–Teller bipolaron that causes additional strain. These observations suggest a rich profile of defects that determine the global electric properties of CCTO thin films as previously reported by other systems [21]. From these results, it can be assumed that the nonlinearity of the system is strongly related to the amount of oxygen and the presence of metal oxide precipitate in the grain boundary which present a "*p*-type semiconductor nature" (metal deficient and oxygen rich phase). In order to understand the phenomena involved in the nonlinearity of the system one should consider that the varistor materials with optimal electrical properties contain an excess of both oxygen and acceptor metal atoms precipitated on the grain boundary surface. The metal atom generally has several oxidation states, which cause the amount of oxygen to increase at the grain boundary. Therefore, the transition metal precipitated at the grain boundary becomes more oxidized when treated in an oxygen rich atmosphere because of the ease with which its valence state changes, causing the electron trapping interfacial region to become richer in oxygen species. It is proposed that the grain boundary region has a "*p*-type semiconductor nature" due to CuO phase precipitated at the grain boundary, while the bulk has an "*n*-type semiconductor nature". This configuration enables electrons to become localized on the surfaces, giving rise to a negative surface interfacial states. To maintain local electrical neutrality, the charges are compensated by ionized shallow donors and bulk electron traps. As a result, electron depletion layers are formed and act as potential barriers which have a Schottky-like nature due to negative interfacial states. Therefore, the physical origin of the interfacial states is not an intrinsic one caused by lattice mismatch at the boundary, but an extrinsic one resulting from metal atoms precipitated at the grain boundaries [22–24].

Complex impedance plots measured at voltages ranging from 1 to 5 V is shown in Fig. 5a for the capacitor. For voltages superior to 1.0 V a single large semicircle is displayed. For voltages higher than 2.0 V, a shoulder develops in the higher frequency range indicating the emergence of a second semicircle. For the second semicircle, a Z_0 value of about 10 Ω has been observed. It has been ascribed to the resistance from cables and probe tips. From these results, the complex impedance plots can be modeled

Table 2 Electrical properties for the $CaCu_3Ti_4O_{12}$ film based varistor sintered at 600 °C for 2 h

Thermal treatment	α	E_b (V cm^{-1})	d (nm)	If (mA cm^{-2})	N_d (m^{-3})	N_{is} (m^2)	ω (nm)	ϕ_b (V)
As—grown	6	203	13	0.08	6.7×10^{25}	1.2×10^{19}	0.8	0.43

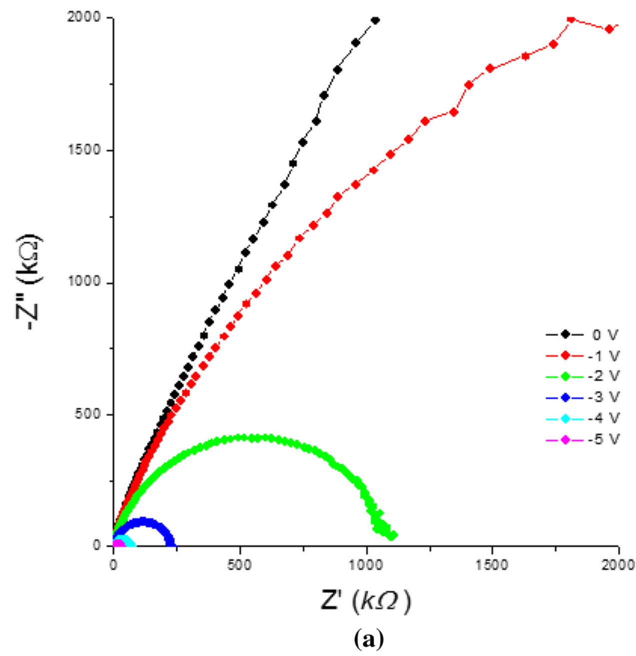

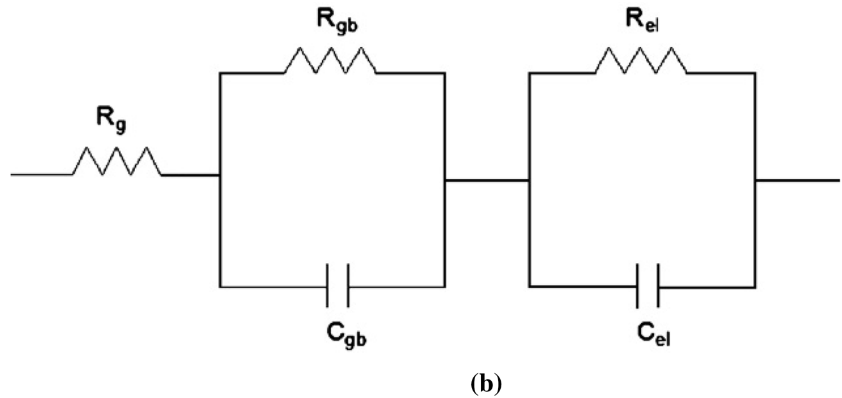

Fig. 5 **a** Complex impedance plot for CCTO thin film deposited by the RF sputtering at room temperature and annealed at 600 °C for 2 h in a conventional furnace and **b** Equivalent circuit model to describe the electrical properties of CCTO thin film

and analyzed using two parallel RC elements, each corresponding to one of the observed semicircles, in series with a connection resistance. These points toward a dielectric response provided by the electrode/CCTO interfaces and not from the CCTO grains. Room temperature interfaces resistance Rint and capacitance Cint were extracted using the relation ωRC = 1. We obtained RintS = 0.1 MΩ mm^2 and Cint/S = 30 nF mm^{-2}. Based on these observations, the CCTO film can be analyzed using the equivalent circuit consisting of a resistor connected in series with two resistor–capacitor (RC) elements as shown in the Fig. 5b, element Rg representing the grain, RgbCgb representing the grain boundary and RelCel representing the electrode–sample interface. Where Rg is the grain resistance. Rgb, Rel and Cgb, Cel are the resistance and capacitance associated with the grain boundary and the electrode–sample interface respectively.

Figure 6a show the Bode complex impedance diagram for the CCTO film. The feature at the highest measuring frequency is characteristic of R–L resonance form, the measuring leads and electrode itself. On the other hand, the region of lower frequencies shows an inverse behavior. This range accounts for grain–grain junctions and controls the global conductivity response, being strongly related to the dielectric mechanism. Moreover, the complex capacitive diagram indicates that the capacitance of the electrodes is hardly affected by the structure of the ferroelectric material. Figure 6b show the Bode capacitive diagrams, confirming the effects of the interface on the capacitance from intermediate to low frequencies. Such a relaxation pattern can be described by an equivalent circuit consistent with three parallel contributions: the “high frequency” limit related to grain boundary capacitances, the complex incremental capacitance at intermediate frequencies related to the relaxation of the particular structure found in the space charge region, and finally, in the low frequency region, the term representing the dc conductance of the multi-junction device. The high frequency region of the

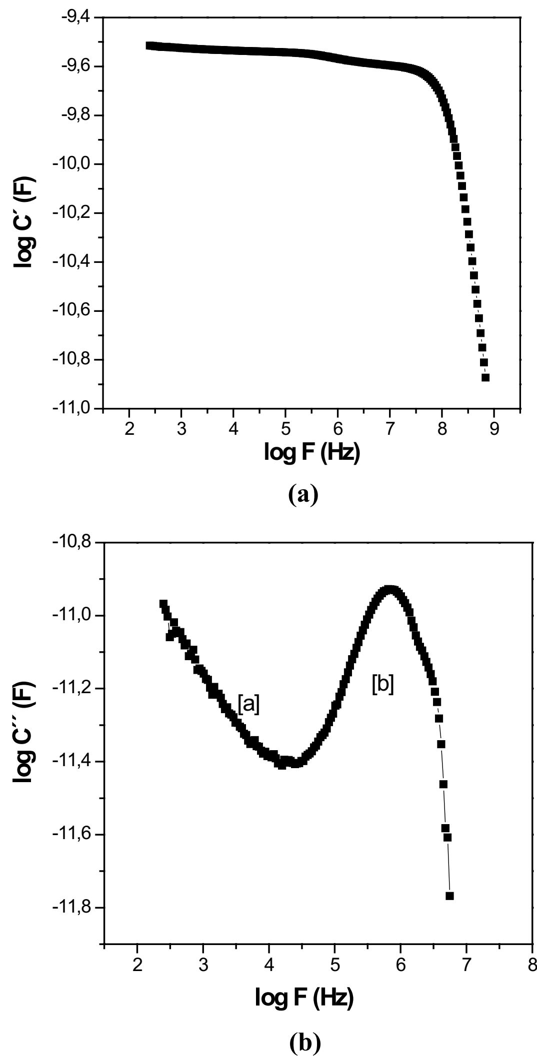

Fig. 6 Bode capacitive diagrams for the CCTO film. Logarithm of **a** real and **b** imaginary parts of the complex capacitance as a function of frequency

complex capacitance diagrams shows the presence of a dipolar relaxation process possessing a near-Debye pattern. It is important to emphasize here that, in the present discussion, because the dielectric properties may be strongly related to a multi-junction domain [25], it is inappropriate to use parameters such as dielectric permittivity or susceptibility, since it is almost impossible to know enough about the geometry, i.e., the thickness of the region in question (domain boundaries existing in the grain), to determine the complex permittivity. That is why we prefer to express the response in terms of complex capacitance (C*) instead of complex dielectric form (ε^*) [26]. Responses due the sample–electrode interfaces which have very high polarization both due the thin film geometry of the interface and the high charge density due to any space charge effects are evident and appear at the lowest measuring frequencies. In the lower frequency region there is a relaxation relating to the grain boundary. This relaxation is probably due to a Schottky-type barrier existing in this type of polycrystalline material. The Bode capacitive diagram provides a better vision of the different relaxations existing in this polycrystalline system and their respective frequency ranges in the CCTO film varistor. Finally, it is now possible to make inferences about the potential barrier formation mechanism in CCTO polycrystalline materials. This mechanism may be similar to the potential barrier formation mechanism proposed for other traditional metal oxide non-ohmic based systems [27]. In other words, a large body of evidence indicates that nonlinear electrical properties arise in non-ohmic devices due to oxygen metal oxide segregation region or precipitated phases. Such a grain boundary region may possess a high “*p*-type semiconductor nature” (metal deficient and oxygen rich) phase compared with the *n*-type semiconductor nature of the grains. For practical varistors applications, we consider the grain boundary region with an excess of both oxygen and acceptor metal atoms precipitated, similar to the other typical varistor ZnO and SnO_2 systems. For instance, we suggested that the CCTO film consisted of semiconducting grains and insulating grain boundaries, which were induced by a small amount of oxygen loss at elevated temperature and limited reoxidation during cooling stage in air. In fact, copper-oxide segregation at grain boundaries are responsible for the insulating properties in such region. Although the compositional inhomogeneity and surface roughness caused by copper-oxide segregation can be a potential problem in thin films, there have been no reports on the effects of copper-oxide segregation on the surface morphology and electrical property of CCTO thin films.

4 Conclusions

We have obtained polycrystalline CCTO thin films by the RF sputtering on $Pt/Ti/SiO_2/Si$ (100) substrates at a room temperature followed by annealing at 600 °C for 2 h in a conventional furnace with a cubic structure belonging to the *Im*-3 space group. The current density–electric field characteristics were found to be associated mainly with the change in the grain boundaries resistivities due to CuO phase precipitated at the grain boundary enabling electrons to become localized on the surfaces. The charge transfer between $[TiO_5{\cdot}V_O^{\bullet}]$ clusters and Cu'_{Cu} defects creates positive and negative polarons and the combination of both constitutes a new entity called Jahn–Teller bipolaron that causes additional strain. The physical origin of the interfacial states at the boundary is a result of metal atoms precipitated at the grain boundaries leading to non-ohmic properties of CCTO film varistor.

Acknowledgements The financial support of this research project by the Brazilian research funding agency FAPESP (Grant No. 2013/07296-2) is gratefully acknowledged.

References

1. D.R. Clarke, Varistor ceramics. J. Am. Ceram. Soc. **82**, 485–502 (1999)
2. S.Y. Chung, I. Kim, S.L. Kang, Strong nonlinear current–voltage behaviour in perovskite-derivative calcium copper titanate. Nat. Mater. Lett. **3**, 774–776 (2004)
3. D.C. Sinclair, T.B. Adams, F.D. Morrison, A.R. West, $CaCu_3Ti_4O_{12}$: one-step internal barrier layer capacitor. Appl. Phys. Lett. **80**, 2153–2155 (2002)
4. L. Mei, H. Hsiang, Effect of copper-rich secondary phase at the grain boundaries on the varistor properties of $CaCu_3Ti_4O_{12}$ ceramic. J. Am. Ceram. Soc. **91**, 3735–3737 (2008)
5. J. Li, M.A. Subramanian, H.D. Rosenfeld, C.Y. Jones, B.H. Toby, A.W. Sleight, Clues to the giant dielectric constant of $CaCu_3Ti_4O_{12}$ in the defect structure of $SrCu_3Ti_4O_{12}$. Chem. Mater. **16**, 5223–5225 (2004)
6. T.B. Adams, D.C. Sinclair, A.R. West, Decomposition reactions in $CaCu_3Ti_4O_{12}$ ceramics. J. Am. Ceram. Soc. **89**, 2833–2838 (2006)
7. S.Y. Chung, I.D. Kim,S.J.L. Kang, Strong nonlinear current–voltage behaviour in perovskite-derivative calcium copper titanate. Nat. Mater. **3**, 774–778 (2004)
8. C.C. Homes, T. Vogt, S.M. Shapiro, S. Wakimoto, M.A. Subramanian, A.P. Ramirez, Charge transfer in the high dielectric constant materials $CaCu_3Ti_4O_{12}$ and $CdCu_3Ti_4O_{12}$. Phys. Rev. B **67**, 092106 (2003)
9. L. He, J.B. Neaton, M.H. Cohen, D. Vanderbilt, C.C. Homes, First-principles study and lattice dielectric response of $CaCu_3Ti_4O_{12}$. Phys. Rev. B **65**, 214112 (2002)
10. E.R. Leite, A.M. Nascimento, P.R. Bueno, E. Longo, J.A. Varela, The influence of sintering process and atmosphere on the non-ohmic properties of SnO_2 based varistor. J. Mater. Sci. Mater. Electron. **10**, 321–327 (1999)
11. V.C. Sousa, M.R. Cássia-Santos, C.M. Barrado, M.R.D Bomio, E.R. Leite, J.A. Varela, E. Longo, Effect of atmosphere on the electrical properties of TiO_2–SnO_2 varistor systems. J. Mater. Sci. Mater. Electron. **15**, 665–669 (2004)
12. S.Y. Chung, I.D. Kim, S.J.L. Kang, Strong nonlinear current–voltage behaviour in perovskite-derivative calcium copper titanate. Nature **3**, 774 (2004)
13. R.A. Young, A. Sakthivel, T.S. Moss, C.O. Paiva-Santos, DBWS-9411—an upgrade of the DBWS*.* programs for Rietveld refinement with PC and mainframe computers. J. Appl. Crystallogr. **28**, 366–367 (1995)
14. P. Jha, P. Arora, A.K. Ganguli, Polymeric citrate precursor route to the synthesis of the high dielectric constant oxide $CaCu_3Ti_4O_{12}$. Mater. Lett. **57**, 2443–2446 (2003)
15. C.R. Foschini, Tararam R., A.Z. Simões, L.S. Rocha, C.O.P. Santos, E. Longo, J.A. Varela, Rietveld analysis of $CaCu_3Ti_4O_{12}$ thin films obtained by RF-sputtering. J. Mat. Sci. Mat. Electron. **27**(1), 2175–2182 (2016)
16. T. Li, R. Xue, J. Hao, Y. Xue, Z. Chen, The effect of calcining temperatures on the phase purity and electric properties of $CaCu_3Ti_4O_{12}$ ceramics. J. Alloy Compd. **509**(3), 1025–1028 (2011)
17. C.R. Foschini, R. Tararam, A.Z. Simões, M. Cilense, E. Longo, J.A. Varela, $CaCu_3Ti_4O_{12}$ thin films with non-linear resistivity deposited by RF-sputtering113, J. Alloy Compd. **574**, 604–608 (2013)
18. J.F. Moulder, W.F. Stickle, P.E. Sobol, K.D. Bomben, *Handbook of X-ray Photoelectron Spectroscopy*, (Perkin-Elmer Corporation, Physical Electronis Division, Eden Prairie, 1992)
19. P.R. Bueno, R. Tararam, P. Parra, E. Joanni, J.A. Varela, A polaronic stacking fault defect model for $CaCu_3Ti_4O_{12}$ material: an approach for the origin of the huge dielectric constant and semiconducting coexistent features. J. Phys. D Appl. Phys. **42**(5), 1–9 (2009)
20. G. Deng, N. Xanthopoulos, P. Muralt, Chemical nature of colossal dielectric constant of $CaCu_3Ti_4O_{12}$ thin film by pulsed laser deposition. Appl. Phys. Lett. **92**, 172909 (2008)
21. L. Ramajo, R. Parra, J.A. Varela, M.M. Reboredo, M.A. Ramirez, M.S. Castro, Influence of vanadium on electrical and microstructural properties of $CaCu_3Ti_4O_{12}$/$CaTiO_3$. J. Alloy Compd. **497**, 349–353 (2010)
22. R. Parra, R. Savu, L.A. Ramajo, M.A. Ponce, J.A. Varela, M.S. Castro, P.R. Bueno, E. Joanni, Sol–gel synthesis of mesoporous $CaCu_3Ti_4O_{12}$ thin films and their gas sensing response. J. Solid State Chem. **183**, 1209 (2010)
23. P.R. Bueno, R. Tararan, R. Parra, E. Joanni, M.A. Ramírez, W.C. Ribeiro, E. Longo, J.A. Varela, A polaronic stacking fault defect model for $CaCu_3Ti_4O_{12}$ material: an approach for the origin of the huge dielectric constant and semiconducting coexistent features. J. Phys. D Appl. Phys. **42**, 055404 (2009)
24. T.T. Fang, C.P. Liu, Evidence of the internal domains for inducing the anomalously high dielectric constant of $CaCu_3Ti_4O_{12}$. Chem. Mater. **17**, 5167–5171 (2005)
25. J. Li, A.W. Sleight, M.A. Subramanian, Evidence for internal resistive barriers in a crystal of the giant dielectric constant material: $CaCu_3Ti_4O_{12}$. Solid State Commun. **135**, 260–262 (2005)
26. A.K. Jonscher, Dielectric characterisation of semiconductors. Solid State Electron. **33**, 737 (1990)
27. P.R. Bueno, E.R. Leite, M.M. Oliveira, M.O. Orlandi, E. Longo, Role of oxygen at the grain boundary of metal oxide varistors: a potential barrier formation mechanism. Appl. Phys. Lett. **79**, 48–50 (2001)